"THE SOURCE MECHANISM OF THE SEISMIC EVENTS DURING THE SEQUENCE OF THE MODERATE-SIZE CRUSTAL EARTHQUAKE OF NOVEMBER 22, 2014 OF VRANCEA REGION (ROMANIA) "

Andreea Craiu*,[1], Cristian Ghita[1], Marius Craiu[1], Mihail Diaconescu[1], Marius Mihai[1], Luminita Ardeleanu[1]

[1] National Institute for Earth Physics, Ilfov, Romania

ABSTRACT

The moderate-size earthquake (ML 5.7) which occurred on November 22, 2014 in Vrancea region (Romania), is the largest crustal event instrumentally recorded. Its aftershock sequence lasted around 70 days, 222 earthquakes with $M_L \geq 0.1$ being located using the records collected by the Romanian seismic network.

The seismic sequence occurred mainly in the lower crust (depths greater than 25 km), and the epicenter distribution - along a NNE-SSW direction - follows the orientation of the Vrancea crustal earthquakes alignment.

The spatio-temporal distribution of the seismic activity, as well as the seismic energy release during the seismic sequence are analysed in detail, and the focal mechanisms of the largest events - 34 shocks with local magnitude ≥ 1.8 - are determined using reliable P-wave polarities and amplitude ratios. Taking into consideration that the moderate-size shock on November 22, 2014 is the strongest instrumentally recorded crustal earthquake in the region, its focal mechanism provides highly relevant seismological information on the deformation field in front of the Carpathian bend. The obtained fault plane solution indicates normal faulting with a dominant dip-slip component; both nodal planes being oriented NW-SE.

1. INTRODUCTION

Vrancea crustal seismic area (Figure 1b,3) of the Carpathians foredeep is characterised by a complex tension field, creating a transition zone from a dominant compresional regime in Vrancea intermediate-depth area, to an extensional regime in the Moesian Platform [Ardeleanu et al., 2005; Popescu and Radulian, 2001].

The crustal seismicity associated with Vrancea seismic region is distributed towards east from the Carpathian Bend in a small band delimited by the Peceneaga Camena fault in the northern part (here was produced the seismic sequence studied in this paper) and the Intra-Moesian fault in the southern part. The crustal seismicity does not exceed $M_W = 5.6$ and apparently hasn't got any connection with the seismic activity from the subducted lithosphere. This seismic activity is characterized by several groups in space and time, seismic sequences in Ramnicu Sarat area and through the seismic sequences and swarms occurred in Vrancioaia area,
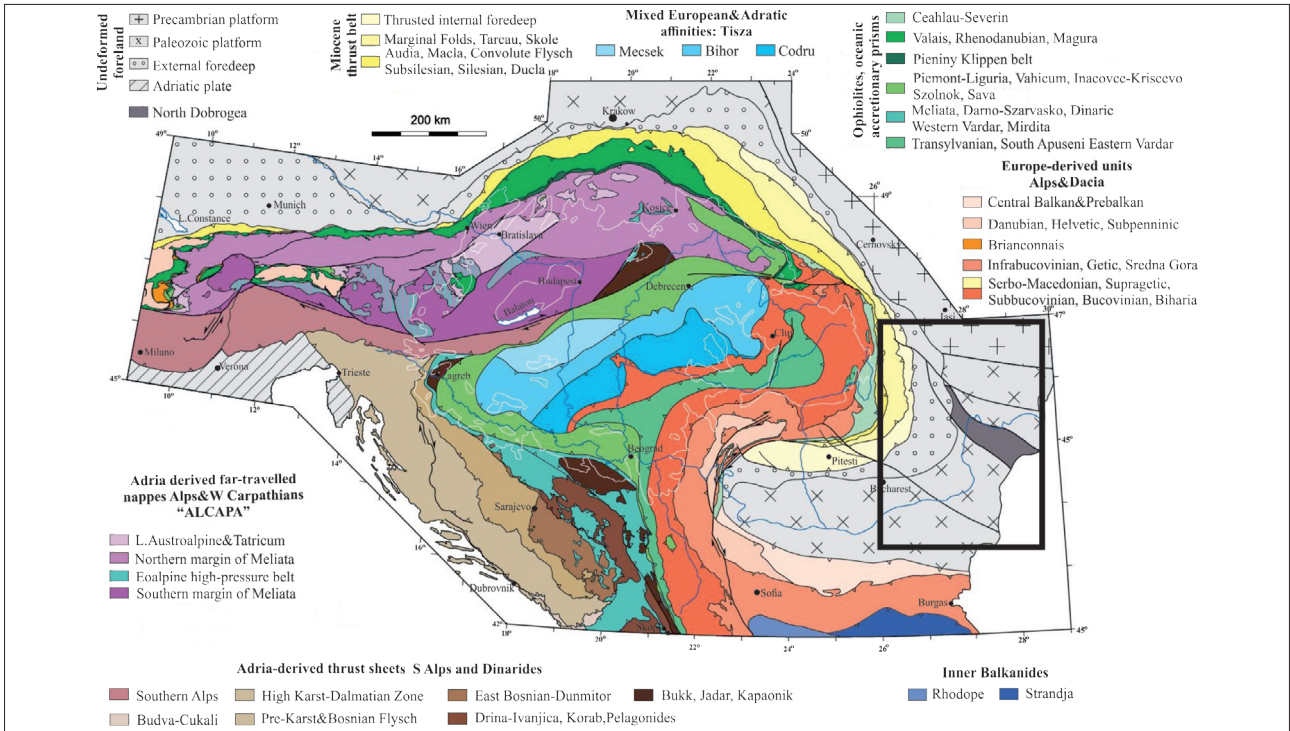
FIGURE 1a. Tectonic map of the Alps-Carpathians-Dinaric system [Schimd et al., 2008]. The inset is the areal of interest for this paper, Figure.1b.
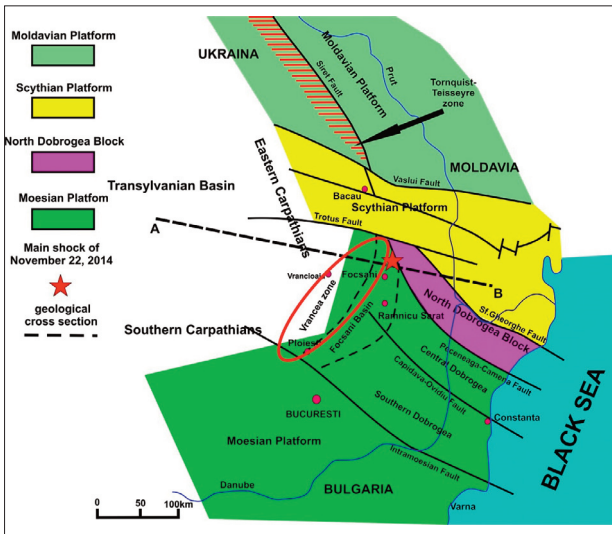

FIGURE 1b. Tectonic map in front of the SE Carpathians (modified after Badescu, [2005]). The yellow star corresponds to the epicenter of the November 22, 2014, crustal earthquake. The AB line corresponds to the tectonic cross section presented in Figure 2.

through the main shocks of the seismic sequences also followed by aftershocks or seismic swarms, [Oncescu and Apolozan, 1984; Oncescu and Trifu, 1987; Popescu E., 2000; Popescu E. et al., 2003; Popescu E. et al., 2012; Tugui et al., 2009]. The earthquakes in the Vrancea region are frequently generated in sequences of small to moderate magnitudes [Tugui et al., 2009]. Constantin et al. [2016] evaluated the results of the macroseismic survey and draw conclusions on the implications for seismic hazard assessment in Romania for the same seismic sequence studied in this paper.

The last sequence occurred in the region in November 2014 was triggered by the main shock on 22 November (ML = 5.7), followed by 221 aftershocks that could be observed until January 30, 2015 ($0.1 \leq M_L \leq 4.5$), this is the only seismic sequence occurred in this area that has focal mechanisms solutions available.

Taking into consideration that the moderate-size shock of November 22, 2014 is the strongest instrumentally recorded crustal earthquake in the region, the main objective of this study is to investigate the source mechanism of this seismic sequence.

2. GEOLOGICAL AND SEISMOTECTONIC SETTINGS OF THE AREA

The Vrancea area is situated in the southern part of Eastern Carpathians and have an intracontinental intermediate-depth seismicity. Beside this one, is also a crustal sesimicity to the east from Vrancea areal in Focsani basin which is partially superimposed over Vrancea in-

termediate-dept earthquakes interval. In the world there are few places with earthquakes at intermediate depths, far from the plate boundaries such as: Bucamaranga in Columbia, the Hindu Kush region nearby to the collision zone between Indian and Euroasian Plates and Vrancea Romania [Zadeh et al., 2012]. The crustal seismicity is disipated in an extension of the Vrancea zone to the Focsani Basin following a distribution of a NE to SW direction (Figure 1b). Even the intermediate and depth earthquakes show a compressive regime (reverse faulting with vertical extension) instead the crustal earthquakes show an extensional regime with normal and strike slip faulting [Radulian et al., 2000 and Tugui et al., 2009; Craiu et al., 2016]. This type of focal mechanisms explaine a slab pulls process wich controll the kinematics of the orogenic system [Zadeh et al., 2012].

The area of interest is situated in the underformed foreland of the Eastern Carpathians (Figure 1a), part of the Alps -Carpathians-Dinaric orogenic sytstem [as described by Schmid et al., 2008]. The units, which form the northern and eastern foredeep of Alps and Carpathians ("External Foredeep"), are partly covered by a little or non-deformed Mesozoic to Cenozoic cover. The East European (is known on the Romanian territory as the Moldavian platform) and Scythian platforms were essentially consolidated in Precambrian times while the Moesian platform underwent significant Variscan deformation. The most external units of the allochthonous Miocene flysch belt of the East Carpathians later partly overrode the Tornquist-Teisseyre Line. The Cimmerian North Dobrogea orogen [Seghedi, 2001] occupies a special position within the Alps-Carpathians-Dinarides system. Along this SE-most segment of the Tornquist-Teisseyre Line (Figure 1b.) the Moesian platform and North Dobrogea orogen were welded along the Peceneaga-Camena Fault Zone before the end of the Early Cretaceous [Hippolyte, 2002] when intense tectonic activity stopped. Both units are separated by the pre-Neogene Trotus fault from the Scythian platform [Săndulescu et al., 1988]. With respect to the post-Early Cretaceous tectonic activity, the North Dobrogea orogen, Moesian and Scythian platforms may be considered as "undeformed foreland" [Schmid et al., 2008]. We prefer to use the term of North Dobrogea block, because even is at the origin an orogen [Seghedi, 2001] nowsday is considered part of an underformed foreland [Schmid et al., 2008].

The area of the 22 November sesimic sequence is situated nearby the contact between three main tectonic units of Romania. The Scythian Platfom, Moesian Plat-

form and the North Dobrogea Block (basically the North Dobrogea Promontory, which represents the prolongation to the west of Danube river, the formations of the North Dobrogea Block).

The southern limit of the Scythian Platform is materialized by Trotus fault with WNW-ESE direction, and from its convergence with Sf. George Fault; the southern limit of the platform follows the direction of this last fault. The Trotus Fault puts in contact the southern part of the Scythian Platform with the Moesian Platform and with the North Dobrogea Block. The Trotus fault cuts off northern part of Peceneaga-Camena fault and Capidava-Ovidiu fault.

Peceneaga Camena fault (PCF) is a transcrustal fracture oriented NW-SE. This fault put in contact Moesian Platform (Central Dobrogea compartment) with the North Dobrogea Block. Over its surface Mohorovicic suffered a vertical lift of Moesian Platform (about 10 km) [Radulescu et al., 1976]. PCF it was also identified on the Black Sea shelf and is marked by epicenters. Before the Cenomanian take place the independent translation, senestra, of the North Dobrogea in relation to Platform Moesian, along a system of horizontal sliding plane which materializes in the Carjelari-Ceamurlia complex [Antonescu and Baltres, 1998]. Peceneaga-Camena fault represent the southern limit of the North Dobrogea block.

Capidava-Ovidiu fault (COF) is also known as Palazu fault. This crustal fault, oriented NW-SE, have a dextral horizontal displacement character. It also separates, in the Platform Moesian, two compartments with different basement and sedimentary covers: a northern compartment (Central Dobrogea) and a southern one (South Dobrogea). The fault has a transcrustal dimension crossing Conrad discontinuity [Radulescu et al., 1976]. She put in contact the Jurassic deposits of Central Dobrogea formations with Cretaceous deposits of South Dobrogea. In depth it put in contact gneisses of Palazu Great Group, from Southern Dobrogea, with the last term of the green schist (upper Proterozoic). The dimension of the thrust is around of 1-1.5 km [Radulescu et al., 1976].

The seismic sequence occurred in the Focsani Basin, and is related to the normal fault system associated to the Peceneaga - Camena fault (Figure 2). Peceneaga - Camena is a major, seismically active, deep crustal fault, oriented NW - SE -, which separates the Focsani Basin (the deepest basin from Romania, having 17 km depth of sediments), part of the Moesian Platform, from the North Dobrogea. 2001) nowadays is considered part of an underformed foreland [Schmid et al., 2008].
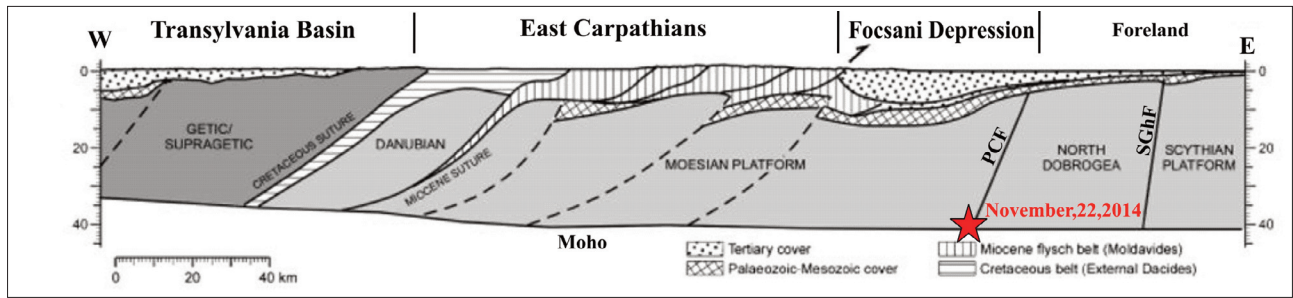
FIGURE 2. Tectonic cross section across the SE Carpathians (after Matenco et al. [2007]) along the line AB in Figure 1. PCF is Pece-neaga-Camena Fault, SGhF is Sfantu Gheorghe Fault.]). The red star corresponds to the hypocenter of the November 22, 2014, crustal earthquake.

3. METHOD

3.1 DATA ACQUISITION, EVENT LOCATION AND MAG-NITUDE ESTIMATION

The recent upgrade of the seismic network in Romania resulted in 158 stations in operation at present (121 in real time), which cover the entire territory (Figure 3). The stations are equipped with high quality digital instruments (Quanterra Q330 or Kinemetrics ROCK digitizers). All the real-time seismic stations transmit the data to the National Institute for Earth Physics (NIEP),

with a sampling rate of 100 samples/sec. At most of the sites, the strong motion acceleration sensors (EpiSensor type) are installed together with broadband velocity sensors (Streckeisen STS2 or Guralp CMG40T).

Real time data is acquired using Antelope software (http://www.brtt.com/software.html). The location algorithm implemented at NIEP uses LocSAT locator and the IASP91 velocity model. For all the events occurred in Vrancea area P and S phases were manually picked in order to get an accurate location. The magnitude for all the events of the seismic swarm was computed us-
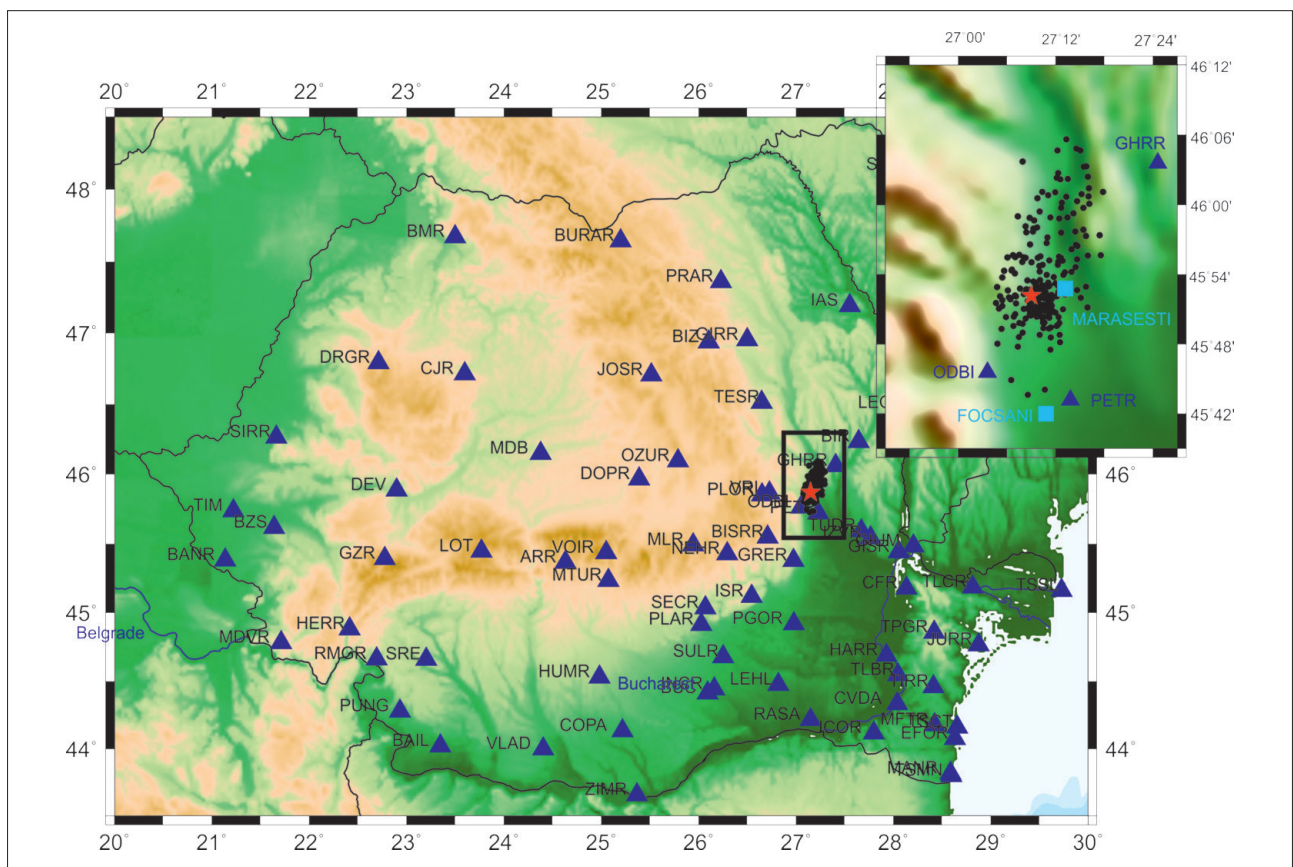

FIGURE 3. Location and epicenters distribution of the seismic sequence recorded in Vrancea zone (Romania), in 2014. Blue triangle- the seismic stations which provided useful data for events location, black circles- earthquakes epicenters and red star – main shock of the seismic sequence.

ing the same relation used for the earthquakes catalogue available at www.infp.ro (independent towards the focal depth) [Richter, 1935], revised by Hutton and Boore [1987]:

$$M_L = \log_{10}(A) + 1.11 \log_{10}R + 0.00189*R - 2.09 \qquad (1)$$

where: A = maximum trace amplitude in nm that is measured on output from a horizontal-component instrument that is filtered so that the response of the seismograph/filter system replicates that of a Wood-Anderson standard seismograph but with a static magnification of 1; R = hypocentral distance in km, typically less than 1000 km. Equation (1) is an expansion of that of Hutton and Boore [1987]. The constant term in equation (1), -2.09, is based on an experimentally determined static magnification of the Wood-Anderson of 2080, rather than the theoretical magnification of 2800 that was specified by the seismograph's manufacturer.

3.2 FAULT PLANE SOLUTIONS

The fault plane solutions of the significant events of the sequence (ML≥1.8) have been obtained on the basis of the first motion of P-wave polarities and amplitude ratios using FOCMEC code developed by Arthur Snoke [Snoke et al., 1984], distributed as part of the FOCMEC package (http://www.geol.vt.edu/outreach/vtso/focmec) and incorporated in SEISAN software [Havskov and Ottemöller, 1999].

The FOCMEC code performs an efficient, systematic search of the focal sphere and reports acceptable solutions based on selection criteria for the number of polarity errors and errors in amplitude ratios [Ottemlöler, Voss and Havskov, 2016].

The search of the focal sphere is uniform in angle, with selectable step size and bounds. Applications have been made to find best-constrained fault-plane solutions for suites of earthquakes recorded at local distances.

The program makes a grid-search and finds how many polarities and amplitude ratios fits each possible solution. All solutions with less than a given number of wrong polarities and/or amplitude ratios within given error limits, are then written out and can be plotted.

Ideally, the solution should be well constrained by polarities only, and then amplitude ratios can provide confirmation of a solution or help to select one of several equally good solutions. The principle behind the amplitude ratio method is that the effect of geometrical

spreading will cancel out when forming the amplitude ratios of S and P waves (or SV/SH) of the same phase type. For event locations and focal plane solutions we used a local velocity model obtained by Koulakov et al., 2010, which has as its grounds the local tomography done by Martin et al., 2006. The values of Q, k, rho used in this study is obtained by Oth et al., 2009.

The parameters of focal mechanisms are given in the two nodal planes (strike, dip and rake for Plane 1 and Plane 2) and P, T axis (azimuth and plunge) following the convention by Aki and Richards [1980].

The solution estimated from P-wave polarities and amplitude ratio was obtained by using no less than 10 observations, therefore its confidence level is considerable, maximum polarities number is 54 for the 22 November 2014 event. The available good quality records allowed us to obtain the fault plane solutions of the earthquakes with local magnitude above 1.8 - the main shock and 32 aftershocks (Table 1).

4. RESULTS AND DISCUSSIONS

4.1 EARTHQUAKES DISTRIBUTION

During the study time interval - November 22, 2014 - February 1, 2015 - 222 earthquakes with $M_L \geq 0.1$ were recorded in the Vrancea crustal-depth source zone; the mainshock had local magnitude 5.7, at 41 km depth. Figure 3 displays the space distribution of the epicenters and the stations of National Seismic Network which provided reliable data for the location of the events sequence.

The set of events is complete for magnitudes larger than 1, as the frequency-magnitude distributions, b value is ~ 0.7 (Figure 4).

The seismic activity has reached a peak in the first 3 days after the mainshock occurrence, while the strongest aftershock, with magnitude 4.5, occurred 15 days later, on December 7, 2014. A new intensification of the activity was observed on December 12, 2014, when two stronger events (local magnitudes 3.1 and 2.6 respectively) were recorded. The significant decrease of the earthquake occurrence rate, noticed after January 3, 2015, was followed by another moderate magnitude aftershock (local magnitude 4.2) which occurred on January 12, 2015, and by a new increase of the seismic activity, which lasted until around February 1, 2015. The daily activities during the whole sequence are shown in Figure 5.

The seismic sequence occurred mainly in the lower crust with depths greater than 25 km and the epicenters

	Date	Time	Lat (°N)	Lon (°E)	H (km)	M_L	Plane 1			Plane 2			P-axis		T-axis		Pol. No./ Err. Pol.	Ratio/ Err. ratio
							Strike	Dip	Rake	Strike	Dip	Rake	Azm	Plg	Azm	Plg		
1	2014/11/22	23:09:58	45.84	27.19	34.9	1.9	339	27	-77	143	64	-97	40	70	238	19	12/2	7/1
2	2014/11/22	20:38:32	45.87	27.18	31.5	2	171	48	85	359	42	96	265	3	31	85	13/1	9/1
3	2014/11/22	19:27:39	45.87	27.15	39.5	2	321	36	-31	77	73	-122	311	52	191	21	10/0	8/1
4	2014/11/22	19:32:36	45.92	27.08	36.7	2.1	334	40	-43	100	64	-122	325	59	212	13	13/0	8/1
5	2014/11/22	22:19:19	45.86	27.17	39.4	2.3	145	74	-20	241	70	-163	103	26	194	2	20/0	11/2
6	2014/11/22	20:24:47	45.87	27.19	40.6	2.8	78	128	-76	257	18	-140	56	54	206	32	28/0	9/0
7	2014/11/22	20:30:56	45.87	27.18	41.0	3.1	130	82	-80	257	13	-142	51	52	211	36	26/2	10/0
8	2014/11/22	19:14:17	45.87	27.17	42.0	5.7	295	15	-106	134	76	-86	50	59	220	31	54/2	11/1
9	2014/11/23	13:01:09	45.83	27.21	39.4	1.8	84	78	-43	185	49	-163	35	38	140	18	11/1	6/0
10	2014/11/23	12:09:27	45.84	26.99	36.1	1.9	339	68	-57	99	39	-143	291	55	45	16	14/0	7/0
11	2014/11/23	00:22:43	45.89	27.02	32.9	1.9	132	62	-38	242	57	-146	95	46	188	4	14/1	7/1
12	2014/11/23	14:47:01	45.87	27.15	33.6	1.9	153	64	39	43	55	147	276	5	11	46	10/0	8/0
13	2014/11/23	04:14:58	45.85	27.16	31.2	2	165	58	-13	262	79	-148	128	30	30	14	18/1	8/1
14	2014/11/23	20:57:59	45.84	27.18	31.7	2	338	33	-79	145	58	-97	34	76	240	13	14/0	7/1
15	2014/11/23	07:03:07	45.85	27.18	45.6	2	345	34	-68	139	59	-104	15	72	240	13	17/0	9/1
16	2014/11/23	05:27:58	45.87	27.18	34.6	2.4	124	52	-69	272	43	-114	93	73	199	5	17/1	7/0
17	2014/11/23	02:21:05	45.87	27.18	37.1	2.5	136	80	-3	226	87	-170	91	9	0	5	24/3	10/1
18	2014/11/23	01:14:39	45.87	27.17	34.8	2.5	114	71	-69	244	28	-137	53	58	188	23	25/0	12/0
19	2014/11/23	04:01:58	45.85	27.18	31.0	2.6	354	50	20	251	75	138	308	16	204	40	24/0	9/1
20	2014/11/23	10:16:14	45.83	27.19	40.5	2.7	132	86	-64	229	26	-172	67	43	199	36	19/0	8/0
21	2014/11/24	23:20:20	45.87	27.18	33.4	2.1	148	52	-85	320	38	-96	85	82	234	7	13/1	9/0
22	2014/11/24	00:45:06	45.88	27.16	34.4	2.4	46	39	-13	146	82	-128	21	40	265	27	24/1	9/0
23	2014/11/25	13:06:42	45.84	27.19	37.5	1.9	329	26	-85	143	64	-92	49	71	235	19	10/1	5/1
24	2014/11/25	01:52:25	45.86	27.16	38.8	3.2	162	68	-51	277	44	-147	117	51	225	14	38/3	11/0
25	2014/12/02	04:19:29	45.89	27.18	29.8	2.5	201	29	55	59	67	107	136	20	358	64	15/0	9/2
26	2014/12/04	05:39:53	45.85	27.20	23.7	2	46	76	-19	141	71	-165	3	24	94	3	10/0	6/0
27	2014/12/07	21:04:05	45.86	27.16	40.6	4.5	126	51	-77	286	41	-105	91	79	207	5	50/0	11/0
28	2014/12/14	18:24:34	45.87	27.09	15.7	2.6	138	79	-45	239	46	-164	88	39	196	20	21/0	10/2
29	2015/01/01	11:39:40	45.85	27.21	31.7	2.2	333	26	-76	138	65	-97	35	69	233	20	13/0	7/0
30	2015/01/12	06:08:31	45.88	27.08	39.4	4.2	116	52	-85	288	38	-96	52	82	202	7	39/2	8/5
31	2015/01/19	23:53:07	45.88	27.13	39.8	3.8	127	28	82	317	62	95	43	17	237	73	41/2	12/0
32	2015/01/20	02:52:46	45.88	27.17	33.4	2.2	302	16	-90	122	74	-90	32	61	212	29	12/1	7/0
33	2015/01/29	12:43:24	45.85	27.18	40.1	2.2	186	86	-84	310	7	-146	103	49	271	41	10/3	7/0

TABLE 1. The focal mechanisms of the seismic sequence of the moderate-size crustal earthquake of November 22, 2014 of Vrancea region.
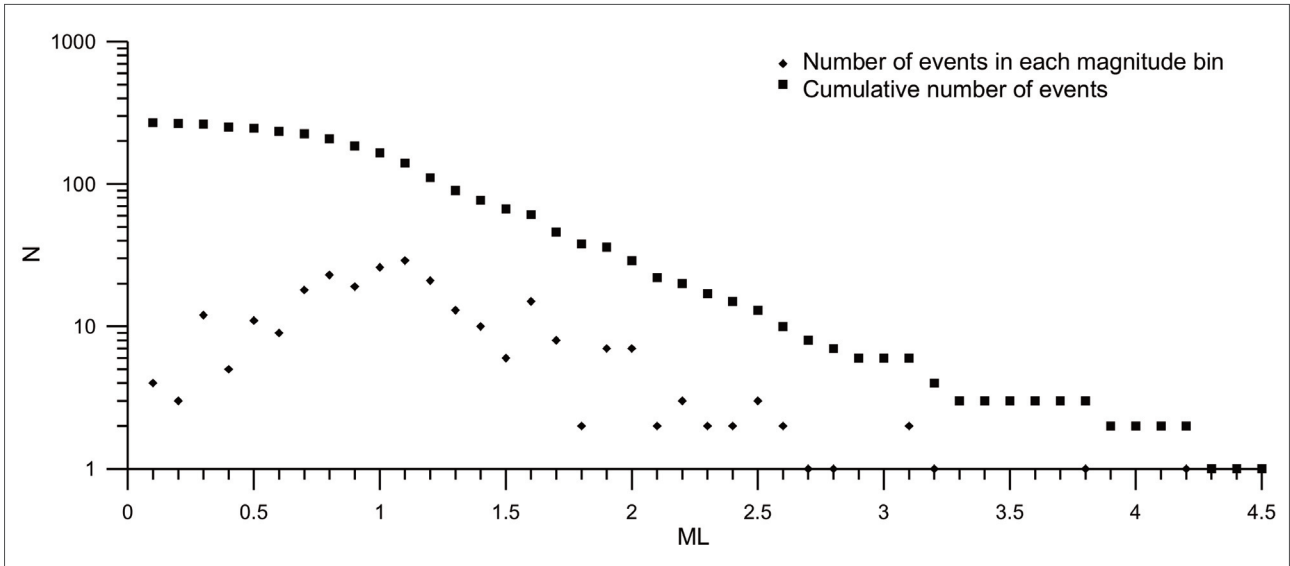
FIGURE 4. The frequency - local magnitude (ML) distribution of the of the studied seismic sequence.

are roughly distributed NNE-SSW (Figure 6).

The aftershocks rate (t) is generally described by the Omori-Utsu law:

$$n(t) = \frac{k}{(c+t)^p} \qquad (2)$$

Where k, c, and p are constants, t is the time since mainshock origin and n(t) is the aftershock frequency measured over a certain interval of time (for a review, see Utsu et al., 1995). Figure 7 shows the decay of aftershock activity in the first 100 days from the mainshock for the stacked earthquake sequences. The pa-

rameters of the Omori-Utsu law (Equation 2) were estimated using a maximum-likelihood procedure [Ogata, 1983]. We found a normal p value (p ˂ 0.96) for the sequences type earthquake activity which is in agreement with Utsu et al., [1995] and other aftershock sequences studies recorded in the vicinity of our area of interest. [Popescu et al., 2000].

4.2 FOCAL MECHANISMS ANALYSIS

The parameters of the focal mechanisms for the major events recorded in the studied seismic sequence are presented in Table 1. All the focal mechanisms are fairly

FIGURE 5. Temporal distribution of the seismic (November 23, 2014- February 1, 2015). Black vertical bars indicate the number of events detected by the stations network in the studied epicentral area, Red vertical bars- number of events with ML>2..
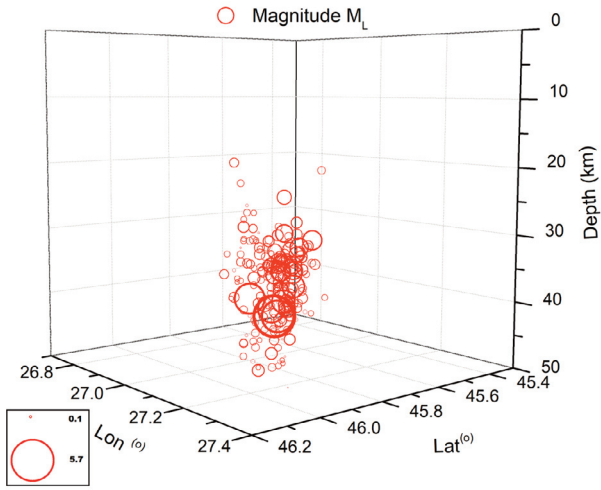
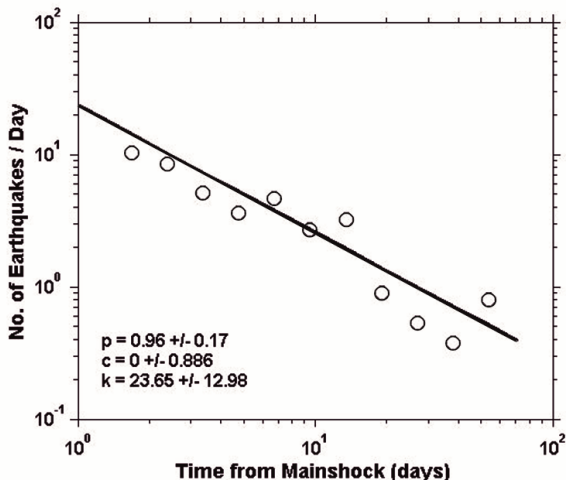FIGURE 6. 3D hypocenters distribution of the seismic sequence.

FIGURE 7. Decay of aftershocks activity versus time for studied sequences. The fit of the data by the Omori–Utsu law (equation 2) and the p, c, and K values, determined as explained in the text, are also given.

well constrained by the available data. They are displayed in Figure 8 and the size of the focal mechanism is scaled by magnitude.

The strongest aftershocks - 2 events with local magnitudes 4.5, and 4.2, respectively - display remarkably similar mechanisms as well. The retrieved fault plane solutions of the weaker earthquakes show certain variability, nevertheless the normal faulting is a common characteristic of most of the shocks with magnitude ≥ 2.5 of the sequence. (Figure 8).

The focal mechanism of the main shock is a normal faulting with a dominant dip-slip component; both nodal planes are oriented NW- SE and is very well correlated with the solutions obtained by several international agencies (INGV, USGS, GFZ, GCMT) Figure 9.
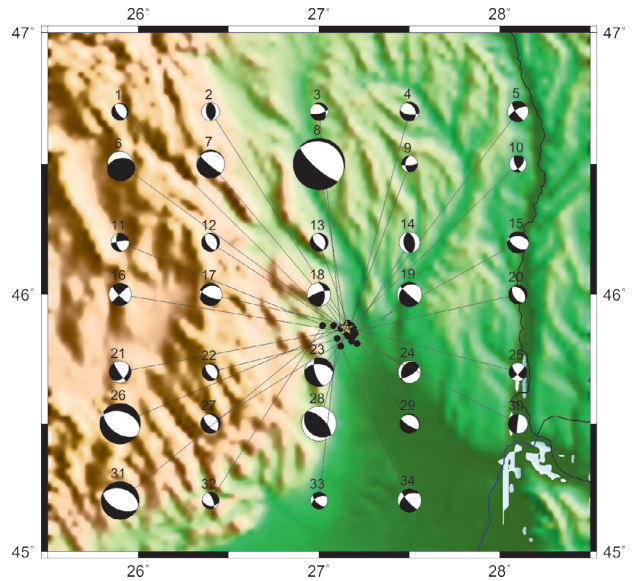

FIGURE 8. The focal mechanisms of the sequence earthquakes with ML≥ 1.8.

In order to represent focal mechanism populations, we proposed a diagram to visualize focal mechanism data as a function of the rupture type. This kind of representation is popular and widely used on seismotectonics to represent the focal mechanism types of the study areas.

To manage and classify focal mechanisms, we used the FMC program [Álvarez-Gómez, J.A., 2014] which produces a type classification [Kaverina et al., 1996]. This approximation began with the use of Frolich Apperson [1992] classification, and improved later on, after Kagan's work [2005] using the 7 earthquake classes proposed by Kaverina [1996]: 1) Normal; 2) Normal -
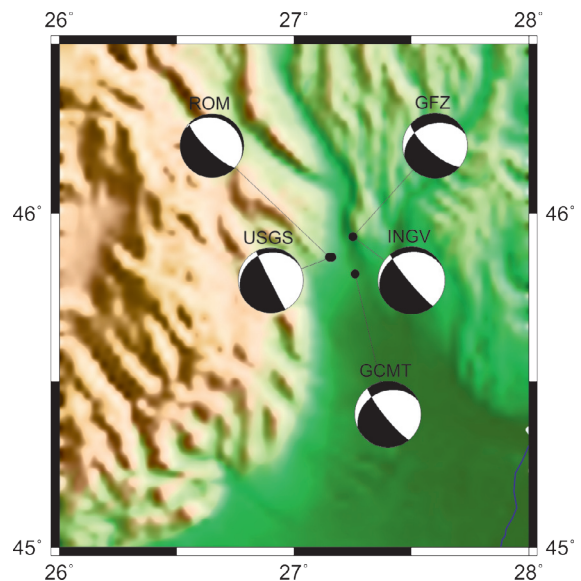

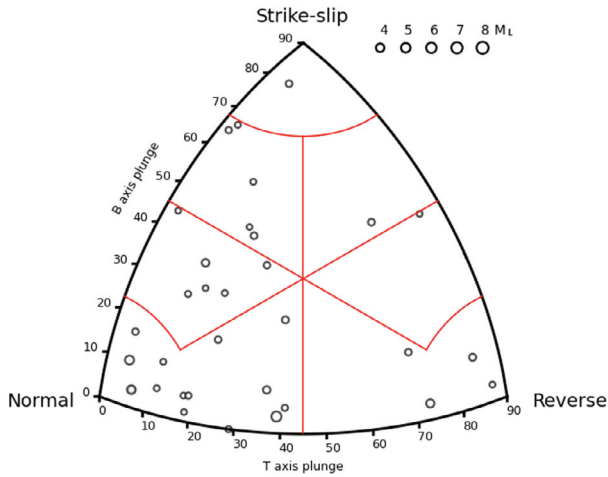FIGURE 9. Fault plane solutions obtained by several international agencies (INGV, USGS, GFZ, GCMT).

FIGURE 10. Focal mechanism classification diagram- Kaverina et al. 1996 projection.

Strike-slip; 3) Strike-slip - Normal; 4) Strike-slip; 5) Strike-slip - Reverse; 6) Reverse - Strike-slip and 7) Reverse. The resulting diagram incorporating 7 fields classification to

the Kaverina projection is shown in Figure 10.

The majority of the fault plane solutions are normal faulting, 6 of them shows a strong strike-slip component. A dominant strike-slip mechanism is observed for the analyzed shock (ML = 2.5), while other 5 events show strike-slip-normal focal mechanism, respectively strike-slip with a noticeable reverse fault component as well (2 events). Five earthquakes show reverse faulting: the 3.8 magnitude aftershock (the nodal planes still orientated SE-NW) and other 4 events with ML≤ 2.6 (Figure 10).

The main axis of the fault plane solutions P and T may show the stress field regime in the seismic zone, in this case indicating a predominant extensional stress field (T plunge is lower than 450, and P plunge in most cases is greater than 450 (Figure 11). The principal axes of the moment tensor presents a fairly high variability in azimuth. It can be observed that the T-axis shows prevailing direction NE-SW, while the P-axis direction is
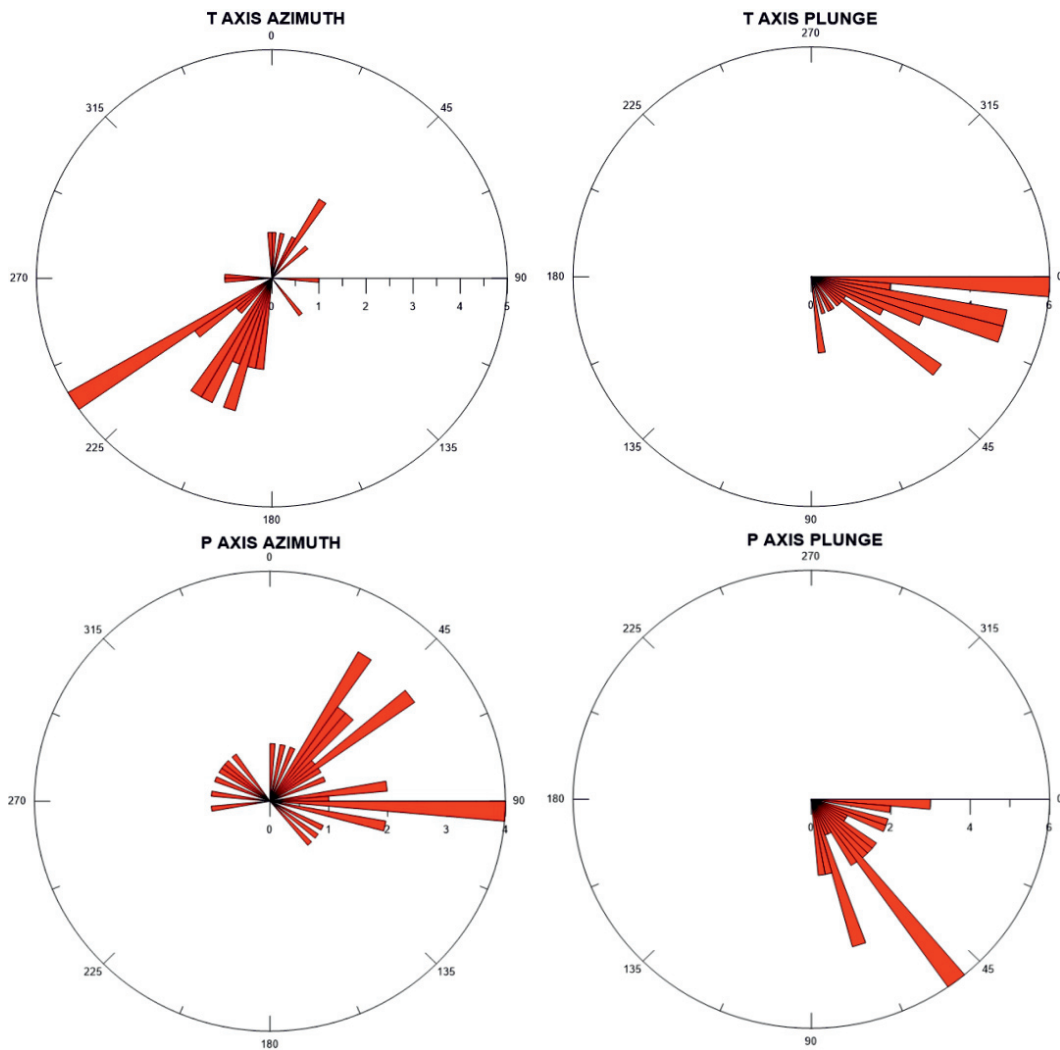

FIGURE 11. Diagrams of the azimuth and plunge of the compression (P) and tension (T) axes of the moment tensor of the investigated seismic sequence.
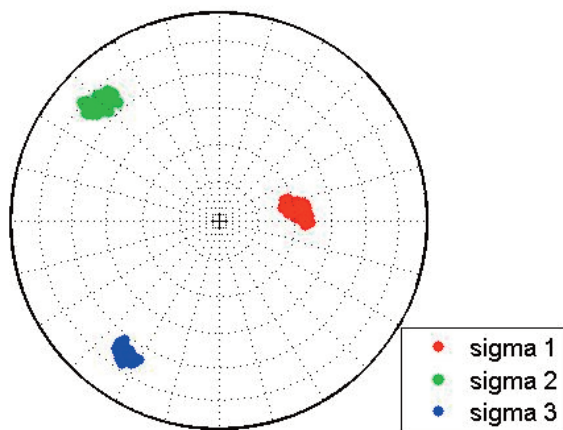
Confidence of principal stress axes

FIGURE 12. Stress direction – confidence limits of the principal stress axes.

Principal stress and P/T axes

FIGURE 13. Focal sphere with the P, T axes and optimum principal stress axes.

more random and shows two prevailing directions NE-SW, respectively, E.

The T axis azimuth group is oriented towards SW which corresponds to the Focsani Basin and meanwhile the P axis azimuth group is oriented towards NE corresponding to the North Dobrogean Promontory and uplift [Matenco et al., 2007; Nastase et al., 2016], the earthquakes occurred on its limit on PC fault having the same orientation NW-SE which explains the majority of the normal earthquakes in this area and especially for this seismic sequence.

To estimate regional stress, we used the program Stressinverse, a code that jointly inverts for stress and fault orientations in [Vavryčuk, 2014].

Stressinverse is a Matlab software package for an iterative joint inversion for stress and fault orientations from focal mechanisms. The inversion is based on Michael's method (1984, 1987) in which an instability criterion proposed by Lund and Slunga [1999] is incorporated.

The stress regime calculated for the region of interest is pure extensive on a NE to SW direction (Figures 12,13).

In the last years several sequences of small to moderate magnitude earthquakes were recorded in the Focşani Basin area [Popescu, 2003]. They show a systematic orientation in NE-W direction, which is parallel to the Carpathian orogen. In many cases the hypocenters are located in the lower crustal domain [Tugui et al., 2009].

Partly, the shallow seismicity follows the alignments at the contact between the major plates colliding in the South-Eastern Carpathians area: the system of major faults oriented NW-SE, separating the Eastern European Plate from Moesian Subplate and the eastern sector from
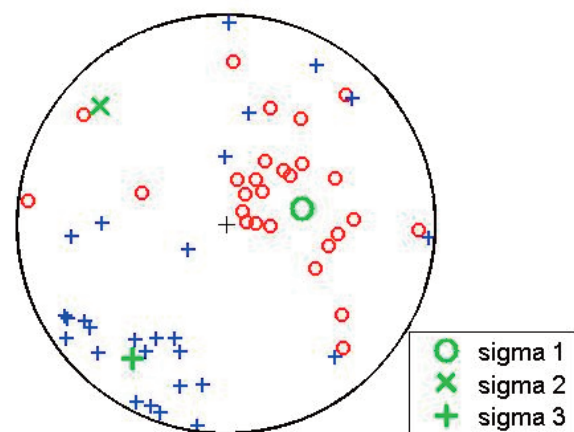
the western sector of the Moesian SupPlate (Trotuş fault, Peceneaga-Camena fault, Intramoesian fault).

The burst of seismicity at the contact between the Focşani Basin and the Carpathians orogen is an expression of the complex collision process that takes place at the South-Eastern Carpathians Arc bending zone. It is difficult to explain at present how the coupling between deformation at depth and deformation in the crust generates earthquake sequences and how these sequences can be related to the generation of major Vrancea subcrustal shocks.

5. CONCLUSION

The moderate-size earthquake with local magnitude 5.7, which occurred on November 22, 2014 in Vrancea region, at 41 km depth, is the largest crustal event instrumentally recorded at the bending of the Eastern Carpathians.

The epicenter distribution for all the sequences in the Vrancea zone (as in the seismic sequence studied in this paper) shows a permanent active alignment oriented NE-SW, parallel to the elongation observed for the hypocenters in the Vrancea subcrustal domain and the principal characteristic of them is the systematic orientation the rupture direction parallel to the orientation of the Carpathians arc [Tugui et al., 2009; Popescu and Radulian, 2001].

However, the stress field is complex in the study area, showing a transition regime from the extensional regime in the Moesian Platform to the compressional regime in the Vrancea subcrustal zone.

The source mechanism of the main shock is a normal faulting with a dominant dip-slip component; both nodal planes are oriented NW- SE and is accordingly with the solutions obtained by several international centers (INGV, USGS, GFZ, GCMT). The strongest aftershocks (M_L = 4.5 and M_L = 4.2) display similar mechanisms, normal faulting with both nodal planes oriented NW-SE. The fault plane solutions determined for the weaker earthquakes show a certain variability; nevertheless, the normal faulting with important strike-slip component dominates among the focal mechanisms of the events of the sequence. The normal faulting is explained by the Focsani Basin subsidence towards the North Dobrogean Promontory [Matenco et al., 2007] and the strike slip component is explained by the total displacement vector as it results from the GPS measurements [Nastase et al., 2016] that shows the relative displacement towards of the Northwestern compartment of the Peceneaga Camena fault the Southwestern compartment.

REFERENCES

Aki K, Richards PG (1980) Quantitative seismology, theory and methods, Vol. I and II. W.H. Freeman, San Francisco.

Álvarez-Gómez, J.A. (2014) FMC: a one-liner Python program to manage, classify and plot focal mechanisms. Geophysical Research Abstracts, Vol. 16, EGU2014-10887.

Antonescu E., Baltres A., (1998). Palinostratigraphie de la Formation de Nalbant (Trias-Jurassique) de la Dobrogea du Nord et des formations jurassiques du sous-sol du Delta du Danube (Plate-forme Scythienne). Geo-Eco-Marina, 3, 159-187

Ardeleanu L, Cioflan C (2005) The seismic sequence of 21-22 February 1983 of Ramnicu Sarat: focalmechanism retrieved by genetic algorithm. Rom J Phys 50(5-6):607-614.

Badescu, D. (2005). The Evolution of the Tectono-Stratigraphy of the Eastern Carpathians During Mesozoic and Neogene Times, Ed. Econ., Bucharest, 308 p. (in Romanian).

Constantin A. P., Moldovan I. A., Craiu A., Radulian M., Ionescu C., (2016) Macroseismic intensity investigation of the November, 2014 M=5.7 Vrancea crustal earthquake, ANNALS OF GEOPHYSICS, 59, 5, S0542; doi:10.4401/ag-6998.

Craiu A., Diaconescu M, Craiu M, Marmureanu A, Ionescu C, 2016, Analysis of the Seismic Activity in the Vrancea Intermediate-Depth Source Region During the Period 2010-2015, The 1940 Vrancea Earthquake. Issues, Insights and Lessons Learnt pp 189-203

Frohlich, C., Apperson, K. D., (1992), Earthquake focal mechanisms, moment tensors, and the consistency of seismic activity near plate boundaries. Tectonics 11 (2), 279-296.

Havskov and Ottemoller, (1999), SeisAn Earthquake analysis software, Seis. Res. Lett., 70, http://www.seismosoc.org/publications/SRL/SRL_70/srl_70-5_es.html

Hippolyte, J.C. 2002: Geodynamics of Dobrogea (Romania): new constraints on the evolution of the Tornquist-Teisseyre Line, the Black Sea and the Carpathians. Tectonophysics 357, 33-53.

Kagan, Y. Y., (2005) Double-couple earthquake focal mechanism: random rotation and display. Geophysical Journal International 163, 1065-1072.

Kaverina, A. N., Lander, A. V., Prozorov, A. G., (1996), Global creepex distribution and its relation to earthquake-source geometry and tectonic origin. Geophysical Journal International 125 (1), 249-265.

Koulakov, I., B. Zaharia, B. Enescu, M. Radulian, M. Popa, S. Parolai, and J. Zschau (2010), Delamination or slab detachment beneath Vrancea? New arguments from local earthquake tomography, Geochem. Geophys. Geosyst., 10, Q03002, doi:10.1029/2009GC002811

Lund, B., Slunga, R., (1999). Stress tensor inversion using detailed microearthquake

information and stability constraints: Application to Olfus in southwest Iceland, J. Geophys. Res. 104, 14.947-14.964.

Matenco L., Bertotti G., Leever K., Cloetingh S., Schmid S.M., Tarapoanca M., Dinu C. (2007) Large-scale deformation in a locked collisional boundary: interplay between subsidence and uplift, intraplate

stress, and inherited lithospheric structure in the late stage of the SE Carpathians evolution. Tectonics 26(TC4011):2007. doi:10.1029/2006TC001951.

Michael, A.J., (1984). Determination of stress from slip data: Faults and folds, J. Geophys. Res. 89, 11.517-11.526.

Michael, A.J., (1987). Use of focal mechanisms to determine stress: A control study, J.

Geophys. Res. 92, 357-368.

Nastase E.I., Muntean A., Toma-Danila D., Mocanu V., Ionescu C. (2016). Study of NW Galati Seismogenic area, 3GPS campaigns from 2013-2015, preliminary results. 5th International Multidisciplinary Scientific GeoConference SGEM 2016, www.sgem.org, SGEM2016 Conference Proceedings, ISBN 978-619-7105-57-5 / ISSN 1314-2704, June 30- July 6, 2016, Vol. 3, 631-639 pp, DOI: 10.5593/SGEM2016/B13

Oncescu M. C., Apolozan L. (1984) The earthquake sequence of Râmnicu Sărat, Romania, of 21-22 February 1983, Acta Geophysica Polonica, 3, 231-238.

Ottemoller, Voss and Havskov, (2016) SEISAN EARTHQUAKE ANALYSIS SOFTWARE FOR WINDOWS, SOLARIS, LINUX and MACOSX.

Oth, A., Bindi, D., Parolai, S., Wenzel, F., S-wave attenuation beneath the Vrancea region (Romania)-new insights from the inversion of Ground Motion Spectra, Bulletin of the Seismological Society of America, DOI: 10.1785/0120080106, 2008.

Popescu, E., (2000), Complex study of the earthquake sequences on the Romanian territory. (PhD Thesis) Institute of Atomic Physics, Bucharest (in Romanian).

Popescu E, Radulian M., Popa M.;Fractal properties of time, space and size distributions of the Sinaia earthquake sequence of May-June, 1993; St. Cerc. Geofizica; 38; 29-39; 2000.

Popescu E, Radulian M (2001) Ramnicu Sarat (Romania) seismic sequence of December 6-8, 1997: source time function and scaling relations of the earthquake parameters. Rom J Phys 46(7-8):515-530.

Popescu E., Popa M., Radulian M., Placinta A. O., (2003) Romanian crustal earthquake sequences: source scaling and clustering peculiarities, St. cerc. Geofizica, tomul 1, p 65-82, Bucharest.

Popescu, E., Borleanu, F., Rogozea, M., Radulian, M., (2012), Source analysis for earthquake sequence

occurred in Vrancea (Romania) region on 6 to 30 September 2008. Rom. Rep. Phys. 64, 571-590.

Rădulescu D., Cornea I., Săndulescu M., Constantinescu P., Rădulescu F. et Pompilian A., 1976, Structure de la croute terrestre en Roumanie, Essai d'interpretation des etudes sismiques profondes, Rev. Roum.Geophys.,5-32.

Radulian M., Vaccari F., Mandrescu N., Panza G.F., Moldoveanu C.L., 2000. Seismic hazard of Romania: deterministic approach. Pure and Applied Geophysics 157, 221-247

Richter CF (1958) Elementary seismology. Freeman, San Francisco

Sandulescu M., Visarion M., (1988). La structure des plate-formes situees dans l\avantpays et au-dessous des nappes du flysch des Carpathe orientales. St.thn. econ. Geofiz.15, 62-67.

Seghedi A., (2001). The North Dobrogea orogenic belt (Romania): a review. In Ziegler P.A., Cavazza W., Robertsone A.F., Crasquin-Soleau S. (Eds.). Peri-Tethys Memoir 6; Peri-Tethyan Rift/Wrench Basins and Passive Margins. Memoires du Museum National d'Histoire Naturelle, 186. Ed. du Museum National d'Histoire Naturalle, Paris, France, pp 237-257.

Schimd S., Bernoulli D., Fugenschuh B., Matenco L., Scefer S., Schuster R., Tischler M., Ustaszewski K., (2008). The Alpine-Carpathian-Dinaridic orogenic system: correlation and evolution of tectonic units. Swiss Journal of Geosciences 101, 139-183.

Snoke, J.A., Munsey, J.W., Teague, A.G. and Bollinger, G. A. (1984) A programme for focal mechanism determination by combined use of polarity and SV-P amplitude ratio data, Earthquake Note, 55, 15pp.

Tugui A., Craiu M., Rogozea M., Popa M., Radulian M., (2009) Seismotectonics of Vrancea (Romania) zone: the case of crustal seismicity in the foredeep area, Romanian Reports in Physics, Vol. 61, No. 2, P. 325-334.

Vavryčuk, V., (2014). Iterative joint inversion for stress and fault orientations from focal mechanisms, Geophysical Journal International, 199, 69-77, doi: 10.1093/gji/ggu224.

Zadeh A. I., Matenco L., Radulian L., Cloething S., Panza G. (2012). Geodynamics and intermediate-depth seismicity in Vrancea (the south-eastern Carpathians): Curent state -of-the art. Tectonophysics 530-531(2012), 50-79

*CORRESPONDING AUTHOR: Andreaa CRAIU,

National Institute for Earth Physics,

Ilfov, Romania

email: atugui@infp.ro